The Effect of Artificial Upwelling on Phytoplankton Dynamics and the Potential for Carbon Sequestration

Joshua Grimstead

May 2025

Abstract

Despite the extensive use of ODE models to explore phytoplankton-nutrient dynamics, Artificial Ocean Upwelling (AU) has rarely been integrated directly into these frameworks. Previous models typically isolate physical drivers, treating upwelling as an external or seasonal nutrient input, rather than modelling it mechanistically. This leaves a gap in our understanding of how AU can alter ecosystem trajectories. Nutrient-Phytoplankton (NP) models that incorporate AU directly offers a tractable yet biologically meaningful approach to explore its ecological effects.

A simple system of externally forced first order ODEs is developed to model phytoplankton growth under AU in temperate oceans particularly during-but not limited to-oligotrophic conditions, which is extended to model carbon sequestration. Initial models consider Mineral-Plant dynamics based on typical population dynamics, before including AU. AU models are then simplified for phytoplankton-nutrient dynamics, which are parametrically forced to include seasonality, and modified to represent carbon sequestration. Seasonality includes phytoplankton blooms and the carbon cycle. Upwelling is assumed to take place in a defined volume of water where the upwelling pump is assumed to have no effect on the system besides the stated upwelling effect.

We show that a general plant-mineral model (not specified to match NP assumptions) yields stable dynamics only when biomass conversion rates are sufficiently high and growth is constrained by crowding and carrying capacity, whereas a simplified NP model achieves stability under low conversion rates through external nutrient input. The NP model captures bloom-like behaviour at higher conversion rates and exhibits oscillations when stratification is included, though sensitivity to parameters limits realism. Upwelling stabilises both models and is predicted to prolong blooms, with implications for phytoplankton-driven carbon sequestration. These findings motivate research into seasonally forced NP models with explicit carbon sequestration and depth structure to better evaluate artificial upwelling as a climate intervention.

1 Background

1.1 Context

According to the most recent predictions, 2025 will see an unprecedented rise in CO_2 levels which will exceed the IPCC 1.5C temperature increase scenarios (in comparison to pre-industrial levels), calling for "immediate and substantial cuts in global CO_2 emissions" in order to change trajectory [1]. As such, carbon dioxide removal (CDR) may prove valuable in conjunction with reducing global emissions to limit global temperature increases, as established by the Paris Agreement.

To meaningfully contribute to climate change mitigation, CDR efforts must be implemented on a massive scale [2], which has prompted research of ocean based CDR approaches. The ocean is the

world's largest carbon sink, "holding roughly 50 times as much inorganic carbon as the pre-industrial atmosphere" and already removes a substantial amount of carbon resulting from human emissions [3].

1.2 Introduction

This paper focuses on Artificial Upwelling (AU), a process in which cool, nutrient rich water from deep ocean regions is transported to the euphotic zone (warmer upper regions that support plant life), prompting growth. Dead plant matter slowly sinks, remineralising the ocean until it reaches a deep anoxic environment (sequestering carbon), or is consumed by other organisms which eventually die and transfer their matter similarly. This process-the biological carbon pump-dictates both the rate of remineralisation, as well as the potential of carbon sequestration.

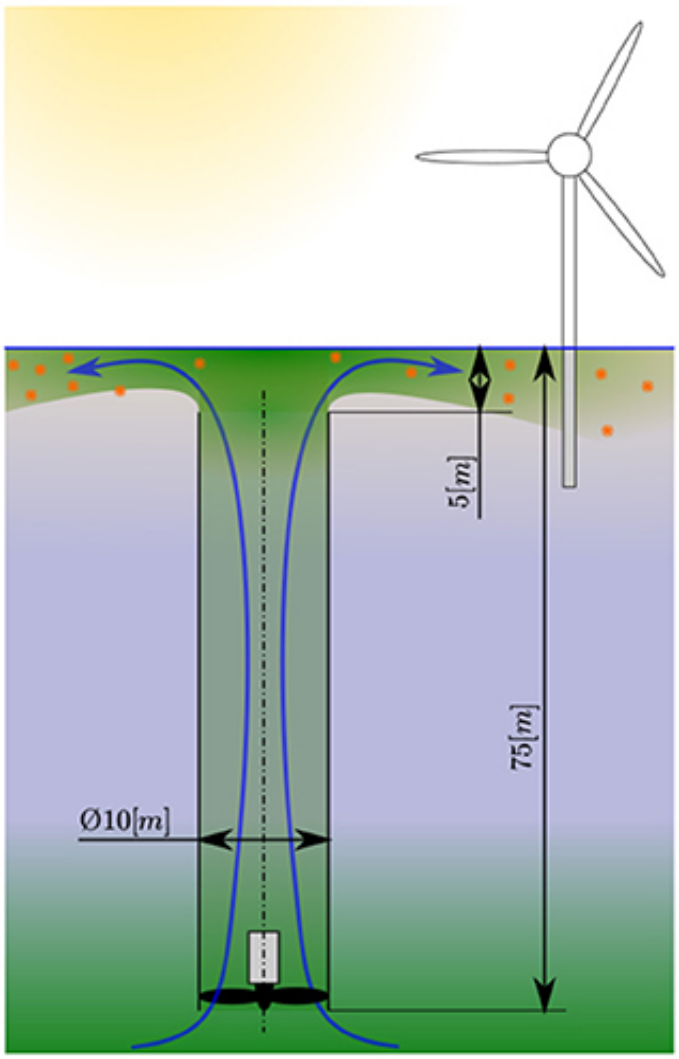

Figure 1: Diagram of artificial upwelling (taken from Suess et. al [9])

Although artificial upwelling is proposed as a method of carbon dioxide removal (CDR), it carries the risk of reintroducing previously sequestered carbon to the surface, potentially leading to a net release of CO_2. Its effectiveness is therefore highly dependent on location, requiring not only nutrient-rich deep waters to support enhanced productivity, but also the capacity for long-term carbon storage, ideally within anoxic or otherwise isolated environments that minimise remineralisation and outgassing.

Phytoplankton population dynamics are typically modelled using coupled first order ODEs, ranging from a system of two equations modelling Nutrient-Plankton (NP) dynamics, to system of four equa-

tions modelling Nutrient-Plankton-Zooplankton-Detritus (NPZD) [4]. Such models demonstrate a range of stability behaviours depending on model complexity and choice of forcing terms. For example, Nutrient-Plankton Models demonstrate osciliatory stability for non-trivial steady states in spring blooms, with linear stability in Autumn Blooms [18] [19].

By contrast, Nutrient-Phytoplankton-Zooplankton (NPZ) and Nutrient-Phytoplankton-Zooplankton-Detritus (NPZD) dynamics result in a hopf bifurcation and forward hysterisis when moving between low and high concentrations of phytoplankton, with bi-stability resulting from multiple attractors (i.e. the inclusion of zooplankton). These dynamics are modified by seasonality forcing terms for light and nutrient disturbances, resulting in unstable conditions. Whilst these models are flexible in approximating multiple biological features, the resulting increases in complexity often decrease interpretability. [4]

Several models have been suggested for artificial upwelling, the most prominent being Earth System Models (ESMs) which simulate the effectiveness of maximum AU deployment, indicating the efficacy of AU is strongly dependent on future emission scenarios [13], and Computation Fluid Dynamics (CFD) using a Reynolds-Averaged Navier-Stokes (RANS) model with the aim of providing insights into the design and efficiency of artificial upwelling systems [9]. Whilst insightful in the physical dynamics of AU, these models do not capture the biological dynamics resulting from upwelling.

While current artificial upwelling models typically isolate biological and physical processes, the incorporation of physical effects into NP-type models is not unprecedented [10], [11]. Both describe the use of forcing terms to modify NP models to include physical effects related to upwelling (fluid dynamics and seasonality). Coupling the biological processes of phytoplankton blooms and the biological carbon pump with the physical process of artificial upwelling enables us to study how artificially stimulated phytoplankton blooms affect ecosystem trajectories and stability, and the capacity of the system for carbon sequestration. This naturally extends to the study of the impact of artificial upwelling under oligotrophic conditions where nutrient delivery is crucial to primary production.

2 Literature Review

2.1 Artificial Upwelling Model and Implementation Results

Current literature on the efficacy of AU as a CDR strategy remains limited. The National Academy of Sciences [12] provides a general overview of the upwelling process, outlining both its theoretical potential and practical limitations [12]. Despite AU being recognised as a possible CDR technique for over 50 years, enhanced oceanic sequestration has yet to be achieved in practice. All documented implementations have been on a small scale and for short durations. Each study underscores the importance of the elemental composition of the source water, alongside considerations of energy utilisation and pumping efficiency as limiting factors. Whilst these limiting factors are important considerations, the conclude that "... in principle and at least in semi-enclosed water bodies where the impact of wind and waves are lessened, AU is a viable means of fertilizing the ocean with growth-limiting nutrients" [12].

Oschlies et al, [13] suggests that AU has a maximum sequestration potential of 0.9 petagrams of carbon a year, whilst > 1 petagrams of carbon needs to be sequestered each year to mitigate anthropogenic carbon emissions [13]. Ocean Iron Fertilisation (OIF), a widely studied CDR technique that adds iron to the oceans to stimulate phytoplankton growth, is suggested to be a more effective and cost-efficient alternative to AU, thus research efforts have been more focused of the implementation of OIF.

Despite several models increasing scepticism regarding the use of AU as a CDR technique due to concerns about both efficacy and cost, the National Library emphasises the need for pilot tests to assess AU efficiency. They note that "ocean physics and biogeochemistry are often more complex and nuanced than can be captured in even the most sophisticated models", highlighting the differing

effects of open ocean and coastal upwelling. A significant gap exists between current models and implementations due to differences in flow rates, indicating that the technological readiness of AU needs to be increased to sufficiently test large-scale implementation [12]. The location of implementation is also a crucial consideration when assessing the permanence of AU carbon sequestration, suggesting different preferred depths depending on model structure.

It is worth noting that, while AU has the potential for carbon sequestration, it may have a net negative effect on the environment due to: energy consumption, potential consequences if the upwelling pump fails, and AU stimulating phytoplankton blooms for offshore fish farming, which has an untested impact on the environment and the overall climate.

Another study, Pan, X., et al [14], discusses hypothetical CO_2 fluxes resulting from simulations or carbonate transformations based on observed carbon and nutrient data in subtropical and tropical oceans off the coasts of Eastern China and Japan. The paper concludes that, despite simulations making assumptions that deviate from reality, AU is a potential CDR technique, capable of turning a carbon source into a carbon sink, assuming the chemical composition of the water permits this. This emphasises the importance of macro-nutrient composition when modelling AU.

Jürchott, et al. [15] highlights further important considerations when modelling AU. The paper examines the effect of AU under different emission scenarios, suggesting that increased plant growth during high emissions scenarios (due to further stratification of ocean layers increasing the prevalence of oligotrophic conditions) resulting in effective sequestration. Conversely, AU during low or no emissions scenarios resulted in outgassing, where AU leads to a net loss of sequestered carbon, responding to changes in model stability due to decreased plant growth. This suggests that AU could prove useful in maintaining a stable level of CO_2 and prevent a greater increase in anthropogenic emissions.

Heinemann, M., et al. [16] primarily investigates the effect of AU intensity on carbon export, using various water column samples to analyse the consistency of sinking sediment and the resulting impact of AU on remineralisation rates. Results indicate that upwelling increased Carbon:Nitrogen ratios, which aids sequestration, and led to a shallower remineralisation depth, implying that remineralisation parameters in an NP model would decrease during AU. In assessing single versus recurring upwelling, the study concludes that recurring fertilisation may result in higher net CO_2 removal due to the export production of an oligotrophic food web. However, conclusions on the effect of AU on carbon sequestration were limited due to the decoupling of biological and physical components. The study stresses the need for monthly to seasonal experimental durations to validate the long-term potential of artificial upwelling for enhanced export production and carbon sequestration, thus supporting the suggested model that couples AU and seasonal phytoplankton dynamics.

2.2 ODE models of phytoplankton dynamics

NP-coupled ODE models have been employed to simulate phytoplankton dynamics since the 1980s, with foundational concepts traceable to as early as 1946 [**?**]. Two recent studies, Kovac [18] and Sharples et al. [19] explore the seasonal dynamics of phytoplankton blooms using NP models. Both papers omits zooplankton dynamics, arguing they are already well studied, and focuses instead on nutrient-phytoplankton interactions. Both studies incorporate a forcing term to model changes in mixed-layer depth, establishing a precedent for coupling physical processes with NP models.

Phytoplankton nutrient uptake in both models is governed by a Michaelis-Menten-type saturation function, $\frac{N}{k+N}$, equivalent to a Holling Type II response [20]. This is used in conjunction with phytoplankton concentration and a light limitation variable, which acts as a dampening effect. However, the models differ in how they represent production: [18] uses detailed equations for daily nutrient production within the mixed layer, whereas [19] adopts a simpler constant per-depth production rate

($r(M)$)based on light availability, serving as an approximation of more complex time-dependent processes, and uses a time-dependent mixed layer deepening rate ($h(t)$) to induce a bloom.

This simpler autumn bloom model is presented below, where:

- P = phytoplankton concentration
- N = nutrient concentration
- M = mixed layer depth
- $r(M)$ = per-depth phytoplankton production rate
- $h(t)$ = mixed layer deepening rate
- N_0 = nutrient concentration in the lower layer
- k = uptake half-saturation constant
- g = per capita mortality rate

$$\frac{dP}{dt} = \frac{N}{k+N} r(M)P - gP - \frac{m+h(t)}{M}P$$
$$\frac{dN}{dt} = -\frac{N}{k+N} r(M)P + \frac{m+h(t)}{M}(N_0 - N)$$
$$\frac{dM}{dt} = h(t)$$

Note that the nutrient equation includes a depth-dependent replenishment term:

$$\frac{m+h(t)}{M}(N_0 - N),$$

modulated by nutrient availability. This introduces a feedback mechanism: when nutrient levels N are already high, the impact of increased mixed layer depth M on nutrient supply diminishes. This reflects the biological intuition that deeper mixing is less effective at enhancing nutrient availability when surface nutrients are already abundant.

A primary difference between the models lies in their treatment of mixed-layer effects. In the spring bloom model [18], light limitation depends on depth but not nutrient concentration, under the assumption that mixing distributes nutrients evenly. The model thus includes a shading dampening mechanism in addition to nutrient limitation. In contrast, the autumn bloom model [19] includes depth as a factor in nutrient dynamics and finds that either gradual or abrupt deepening of the mixed layer prevents blooms from forming.

The spring model further finds that changes in mixed-layer depth lead to new steady states without affecting stability-a result consistent with the Sverdrup critical depth hypothesis [21]. Regardless of whether the layer shallows or deepens, the steady state remains stable.

The spring model, however, did find that a low nutrient supply leads to oscillatory behaviour, whereas higher nutrient supply results in stable, non-oscillatory dynamics. This outcome emerges specifically from the inclusion of a nutrient limitation term in the production function-without it, no oscillations occur, regardless of supply rate. This reveals the counter-intuitive result that deeper, less nutrient-rich layers can sustain more dynamic bloom cycles, while shallower, nutrient-rich layers tend toward stable, saturated states. In the context of artificial upwelling, this suggests that the intervention may be most effective when used to deepen shallow states, allowing higher biomasses to be reached.

As region effects the level of depth, we note the differences between coastal and deep-water phytoplankton blooms. He et al. [22] utilised satellite remote sensing data to analyse the spatial and temporal characteristics of harmful algal blooms (HABs) in China's offshore waters from 1990 to 2019. The research revealed that HABs were predominantly concentrated in coastal regions, particularly in areas with high population density and significant economic development. These coastal zones experienced more frequent and intense blooms compared to offshore areas, a pattern attributed to increased nutrient inputs from river discharges and anthropogenic activities.

The study found that the majority of HABs occurred between April and September, accounting for 88% of the total events from 2009 to 2019. This seasonal peak aligns with warmer temperatures and enhanced nutrient availability during the spring and summer months, which lead to phytoplankton growth. In contrast, offshore regions exhibited fewer blooms, due to lower nutrient concentrations and different oceanographic conditions. This suggests that altering these conditions through AU or similar may result in both an increase in nutrients and a deepening of the mixed layer which will allow for more prominent blooms in off-shore regions, depending on environmental factors such as weather and tides, as well as anthropogenic factors.

Seasonal research indicates that artificial upwelling may be most effective when induced after a natural phytoplankton bloom, particularly under conditions where other requirements for growth (e.g. light and temperature) are already satisfied but nutrients are depleted [23]. Consequently, the impact of upwelling during natural bloom events is expected to be limited, while its potential is significantly greater during oligotrophic periods-such as the post-bloom phase and in summer, when surface nutrient concentrations are typically low.

Thingstad et al. [24] hypothesises that post-bloom AU during oligotrophic periods could lead to a two-stage phytoplankton bloom: an initial diatom bloom supported by nitrate, followed by a bloom of nitrogen-fixing bacteria utilizing the remaining phosphate, supporting the creation of a model that implements AU in an oligotrophic environment post-phytoplankton bloom.

Although summer blooms can occur, their classification as true bloom events remains contested, implying there may be scope for nutrient-driven stimulation via upwelling. Some studies have shown that summer blooms are often associated with specific nutrient limitations-phosphorus, for instance-highlighting the importance of nutrient type in determining the effectiveness of upwelling interventions.

Moreover, different phytoplankton species have distinct bloom requirements [25], including varying sensitivities to light and nutrient availability. This seasonal and species-specific variability in bloom dynamics may influence the effectiveness of artificial upwelling and should be considered when interpreting model outcomes. For simplicity, we see the spring and autumn models [18],[19] assume a single phytoplankton type that exhibits recurrent blooms at predictable times .

2.3 Literature Conclusion and Current Hypothesis

Despite existing reservations, studies such as Heinemann, M., et al.[16] highlight the importance of investigating coupled biological-physical systems. The objective here is to develop a model suited to oligotrophic conditions in deep waters, where artificial upwelling is expected to have the greatest impact. While many existing models incorporate strict assumptions regarding light dynamics and self-shading, these effects have been well explored and will be treated as constant in our approach. Although depth has been shown to influence bloom dynamics, given how these effects are well studied we construct our model under the simplified assumption of a single-layer, closed system. From this foundation, we derive a model from assumptions based on established phytoplankton dynamics and subsequently compare its behaviour with that of existing frameworks.

We hypothesises that Artificial Upwelling, when applied following seasonal nutrient depletion (typically the case in summer or post-bloom conditions) can restore system stability by reintroducing nutrients into an oligotrophic environment. Under these conditions, where light and temperature are assumed sufficient, the limiting factor becomes nutrient availability. However, due to physiological constraints on uptake and saturation thresholds, the resulting phytoplankton blooms are expected to be smaller than those triggered by natural seasonal influxes. Consequently, AU may extend productivity without replicating the intensity of spring blooms.

We anticipate that upwelling will shift the system's steady states, promoting stable biomass levels where decline or oscillations might otherwise occur. At the same time, the potential for carbon sequestration introduces competing dynamics: while nutrient delivery supports biomass growth, it may also raise the risk of destabilisation through remineralisation and feedback loops, particularly in closed systems. As such upwelling must be implemented carefully so as not to induce unrealistic oscillatory behaviour. This study explores these interactions by assuming a single-layer model with constant light conditions, focusing on nutrient dynamics and carrying capacity effects to understand how AU influences bloom stability and carbon storage potential.

3 Initial Plants and Minerals Model

3.1 Initial Model Assumptions and Rationale

Table 1 presents the foundational assumptions of a simplified Plant-Mineral model, developed as a stepping stone toward more complex Nutrient-Phytoplankton dynamics. This initial model focuses on biological and nutrient cycling within a closed, well-mixed upper ocean layer, under assumptions typical of oligotrophic summer conditions where artificial upwelling may have maximal impact. The aim is to capture the core feedbacks between plant growth and nutrient availability without the confounding influence of external or multi-trophic interactions.

Assumptions are categorised by type:

- **Spatial:** Concern the spatial resolution of the model (e.g. homogeneity).
- **Temporal:** Concern how time-dependent processes are included or omitted.
- **Dynamical:** Concern the mathematical structure and behavioural rules of growth, death, and transformation.
- **Biogeochemical:** Concern nutrient cycling, stoichiometry, and remineralisation.
- **Biological:** Concern plant biology, behaviour, and species-level interactions.
- **External:** Assumptions about exogenous factors such as human impact or natural variability.

Assumption	**Assumption Type**	**Strength**	**Model Implication**	**Notes / Clarification**
No temporal forcing (seasonality or diel cycle)	Temporal	Strong	Allows autonomous system of ODEs; no explicit time-dependent parameters	Reflects stable summer conditions with persistent light
No light limitation (implied in seasonal assumption)	Biological	Strong	Light not included as a limiting factor	Appropriate for oligotrophic summer conditions
Closed system	Dynamical	Strong	No input or loss of plant biomass or minerals; total mass conserved	Ensures internal consistency of feedback mechanisms-will be violated when adding upwelling
Constant production/death rate $\propto$ plant population	Dynamical	Strong	Linear mortality terms simplify dynamics	No density or environment dependence included for plant reproduction or mortality

Assumption	Assumption Type	Strength	Model Implication	Notes / Clarification
Instantaneous recycling upon death	Dynamical	Moderate	Immediate return of minerals to mineral pool after mortality	Avoids the need to incorporate a time delay in model formulation
No predation	Biological	Strong	Mortality due to internal processes only	We assume mortality isn't dominated by grazing
Environmental carrying capacity	Biological	Moderate	Puts a hard upper bound on plant density	May be implicit via resource limitation or added explicitly to represent the limit of the defined area
Plant growth and reproduction are equivalent	Dynamical	Strong	No differentiation between new plants and old plants growing	No change in result given both lead to more carbon capture, however at different rates.
Maximum mineral uptake rate per unit time	Dynamical	Strong	Prevents unbounded uptake at high mineral concentrations	Likely to be implemented via saturation kinetics
Redfield-like stoichiometry for uptake and remineralisation	Biogeochemical	Moderate	Allows representation of macronutrient cycling with a single "mineral"	Reflects Redfield's empirical nutrient ratios (C:N:P)
All minerals behave similarly	Biochemical	Moderate	Multi-nutrient complexity collapsed into a single term	Assumes uniform uptake rates and importance
All minerals return on death (no sequestration)	Biogeochemical	Moderate	Closes nutrient loop with full remineralisation	No sinking loss; can be later relaxed
No anthropogenic influence	External	Moderate	Excludes fertilisation, emissions, or direct human impacts	Focus remains on natural dynamics

Table 1: Structured assumptions for the plant-mineral model.

Note the assumption of Redfield-like stoichiometry refers to the near-constant elemental ratios of carbon, nitrogen, and phosphorus observed in phytoplankton and ocean waters, first introduced by Redfield [26]. This enables the reduction of multiple nutrient variables into a single representative "mineral" term without substantial loss of biological realism.

3.2 Exploration of Dynamics

We begin our modelling framework with a set of simplifying assumptions intended to capture the essential features of plant-mineral interactions. Our initial formulation adopts a Lotka-Volterra structure for plant growth, incorporating nutrient uptake and a constant per-capita mortality rate.

Let:

- $M(t)$ = Mineral concentration at time t (mmol m^{-3})
- $L(t)$ = Density of living plants at time t (mmol m^{-3})

- δ = Per capita plant mortality rate ($[t]^{-1}$)
- b = Plant production rate ($[t]^{-1}$)
- t = time ($[t]$)

The basic system is given by:

$$\frac{dL}{dt} = bML - \delta L$$
$$\frac{dM}{dt} = \delta L - bML$$

Note that throughout our models we assume plant production rate b is greater than death rate δ, as a result of our assumption of ideal growth conditions. Also note that the dimension of the time parameter is chosen relative to the current model and as such is unspecified. To account for limitations in environmental resources and spatial constraints, we introduce a carrying capacity K for plants. We also distinguish between the efficiencies of biomass conversion in both directions:

- K = Environmental carrying capacity (mmol m^{-3})
- r = Mineral-to-plant conversion efficiency (dimensionless)
- λ = Plant-to-mineral conversion efficiency (dimensionless)

The system is modified accordingly:

$$\frac{dL}{dt} = rbML\left(1 - \frac{L}{K}\right) - \delta L$$
$$\frac{dM}{dt} = \lambda\delta L - bML$$

Next, we introduce biological limitations on nutrient uptake. Specifically, we incorporate a Michaelis-Menten-style saturation function that reflects the decreasing efficiency of mineral absorption at high concentrations of minerals or high densities of plants as visualised in Figure 2. This leads to:

- α = Half-saturation constant (mmol m^{-3})
- ϕ = Mineral limitation parameter (dimensionless)
- ψ = Plant limitation parameter (dimensionless)

The equations become:

$$\frac{dL}{dt} = \frac{rbML}{\alpha + \phi L + \psi M}\left(1 - \frac{L}{K}\right) - \delta L$$
$$\frac{dM}{dt} = \lambda\delta L - \frac{bML}{\alpha + \phi L + \psi M}$$

Finally, recognising that nutrient availability affects environmental capacity, we allow the carrying capacity to vary dynamically with the mineral concentration according to the dynamics below which are visualised in Figure 3:

$$K(M) = K_0 + (K_1 - K_0)\frac{M}{\gamma + M} \qquad (\dagger)$$

Substituting †into our system, we obtain the full dynamic model (1):

$$\frac{dL}{dt} = \frac{rbML}{\alpha + \phi M + \psi L}\left(1 - \frac{L}{K(M)}\right) - \delta L \tag{1a}$$

$$\frac{dM}{dt} = \lambda\delta L - \frac{bML}{\alpha + \phi M + \psi L} \tag{1b}$$

This establishes the foundation of our plant-mineral interaction model, balancing uptake saturation, resource limitation, and conversion dynamics in a closed system.

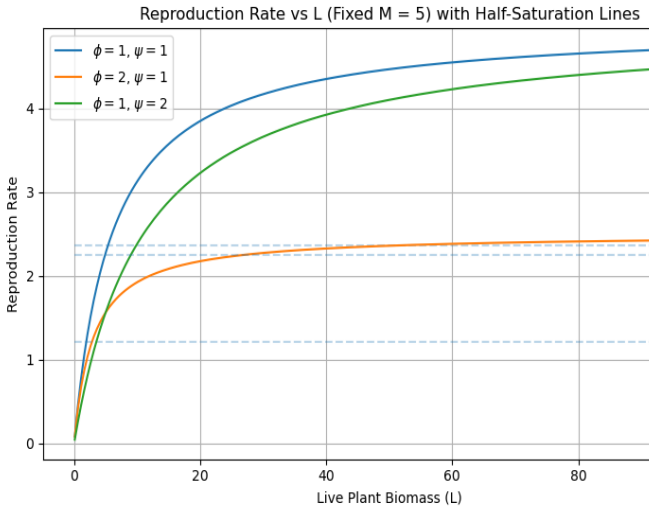

Figure 2: Isolated saturation effect at different saturating values

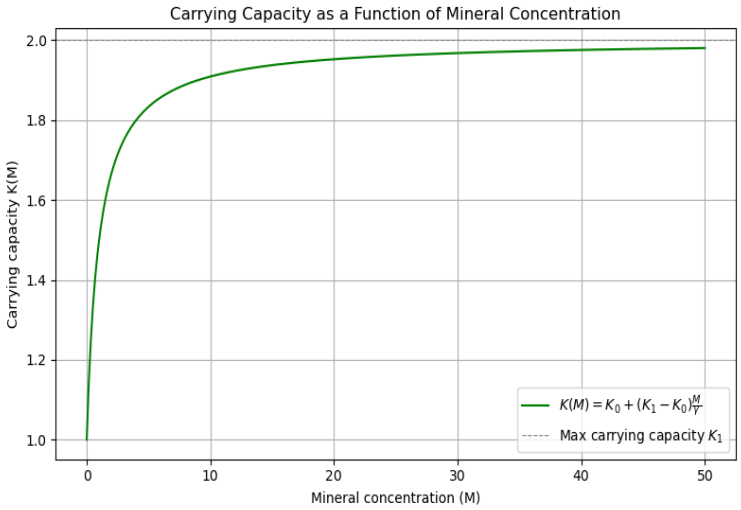

Figure 3: Isolated Carrying Capacity function

The left panel shows the effect of Michaelis-Menten like uptake limitations under different parameter choices for ϕ and ψ. We compare cases where the limitation is symmetric ($\phi = \psi$) and asymmetric ($\phi \neq \psi$), noting how similar increases in variables have notably different results with respect to the parameter choice. Although these graphs fix $L = 5$ for illustration, similar qualitative behaviour is observed when fixing M instead, since these are representative examples rather than fitted data.
The right panel displays how carrying capacity $K(M)$ increases with mineral concentration, with minimum value $K_0 = 1$ and maximum value $K_1 = 2$.

3.3 Graphical Analysis

We conduct initial analysis on system (1) through phase plane portraits at values to visualise how steady states change. Whilst the chosen dynamic carrying capacity †is representative of real world dynamics, we see that our choice of carrying capacity doesn't influence the stability of the steady states, thus to simplify dynamics we assume a constant carrying capacity going forward.
Thus we use the following example parameter choices to visualise the different potential solutions: $b = 3.2$, $\alpha = 0.1$, $\phi = 2.2$, $\psi = 0.4$, $\delta = 0.6$, $\lambda = 1.2$, and constant $K = 5.2$. Figure 4 corresponds to $r = 1.2$, while reducing r to 0.8 produces the unstable behaviour seen in Figure 5.

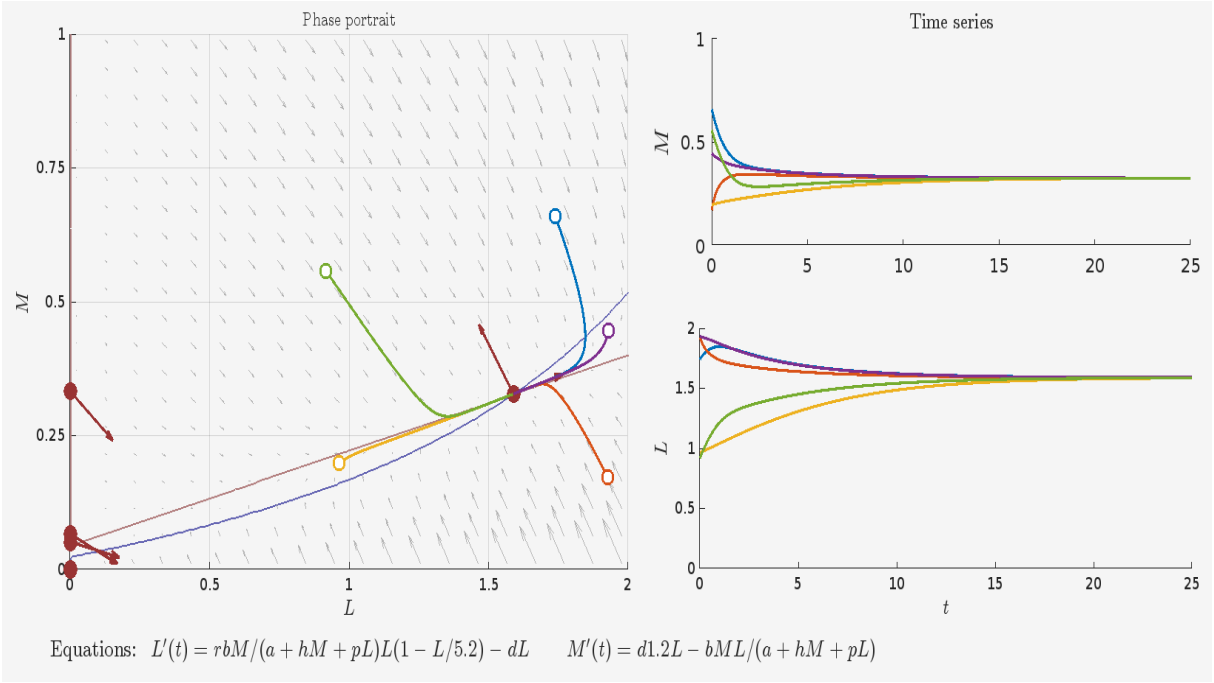

Figure 4: Minerals-Plant Model under stable conditions

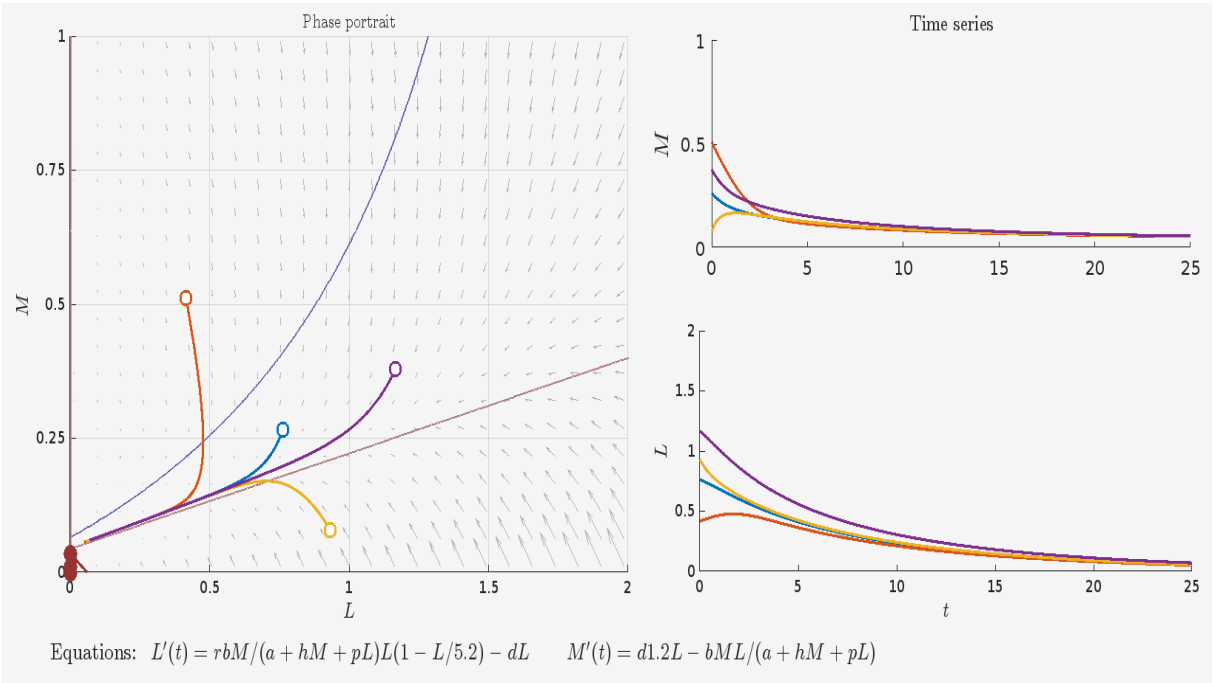

Figure 5: Mineral-Plant Model under unstable conditions

We observe that a change in stability occurs precisely when the threshold $r\lambda = 1$ is crossed. Figure 4 demonstrates a stable node for the non-trivial equilibrium and a line of unstable semi-trivial equilibria via example nodes. In contrast, Figure 5 shows only semi-trivial stability ($r\lambda < 1$). The stability of the equilibrium line changes at the intersection of the semi-trivial equilibrium line $L = 0$ and the minerals nullcline, whereas the intersection of the plant nullcline with the same line does not alter the system's stability. This indicates that the intersection points along the $L = 0$ axis play a key role in determining system stability, which motivates an algebraic investigation into the origins of stability change.

3.4 Algebraic Analysis

We begin by conducting a steady state analysis. Going forward, we assume K is fixed, and consider both cases $\psi = 0$ and $\psi \neq 0$.
Since $L = 0$ is a trivial nullcline for both equations, the M-axis forms a line of equilibrium points. For $L = 0$, the plant and mineral nullclines each intersect the M-axis at specific points. These intercepts determine the local stability along this line.

$$\text{(2a)} \quad M_1 = \frac{\lambda\delta\alpha}{b - \lambda\delta\phi} \quad \text{(Minerals)}$$

$$\text{(2b)} \quad M_2 = \frac{\delta\alpha}{rb - \delta\phi} \quad \text{(Plants)}$$

Note that since ψ only modifies terms involving L, it is irrelevant for this part of the analysis. Here, M_1 refers to the intersection of the minerals nullcline with the M-axis, and M_2 to that of the plants nullcline. While these are not full equilibria, their relative positions directly inform the stability of the semi-trivial steady states. We distinguish three cases based on the relationship between M_1 and M_2, which is governed by the ratio between λ and r:

$$\begin{gathered}(1)\ M_1 = M_2 \text{ if } r = \tfrac{1}{\lambda} \\ (2)\ M_1 < M_2 \text{ if } r < \tfrac{1}{\lambda} \\ (3)\ M_1 > M_2 \text{ if } r > \tfrac{1}{\lambda}\end{gathered}$$

Note we only consider cases where $M_1, M_2 > 0$. This condition is represented through:

$$M_1 > 0 \implies \frac{b}{\lambda} > \delta\phi \qquad M_2 > 0 \implies rb > \delta\phi$$

Thus, we must have biological realism conditional on:

$$\delta\phi < \min\left\{\frac{b}{\lambda}, rb\right\}$$

Next, we analyse the non-trivial steady state by expressing the nullclines in terms of L:

$$M_3 = \frac{\lambda\delta(\alpha + \delta\psi L)}{b - \lambda\delta\phi} \quad \text{(Minerals)}$$

$$M_4 = \frac{\delta\alpha(\alpha + \delta\psi L)}{rb - \delta\phi - \frac{rbL}{K}} \quad \text{(Plants)}$$

For both $\psi = 0$ and $\psi \neq 0$, we derive the non-trivial steady state:

$$\text{(2c)} \quad L^* = \frac{K}{r}\left(r - \frac{1}{\lambda}\right)$$

Substituting this into M_3 gives:

$$\text{(2d)} \quad M^* = \frac{\delta}{\frac{b}{\lambda} - \delta\phi}\left(\alpha + \frac{K}{r}\left(r - \frac{1}{\lambda}\right)\psi\right)$$

Stability Analysis

We define the system as:

$$f(M,L) = \frac{rbML}{\alpha + \phi M + \psi L}\left(1 - \frac{L}{K}\right) - \delta L$$

$$g(M,L) = \lambda\delta L - \frac{bML}{\alpha + \phi M + \psi L}$$

Where the Jacobian of the system is determined using the following format:

$$J = \begin{bmatrix} f_L & f_M \\ g_L & g_M \end{bmatrix}$$

The general result of the partial derivatives is as follows:

$$f_L = -\frac{rbML\psi(1-\frac{L}{K})}{(\alpha + M\phi + L\psi)^2} + \frac{rbM(1-\frac{L}{K})}{\alpha + M\phi + L\psi} - \delta - \frac{rbML}{K(\alpha + M\phi + L\psi)}$$

$$f_M = -\frac{rbML\phi(1-\frac{L}{K})}{(\alpha + M\phi + L\psi)^2} + \frac{rbL(1-\frac{L}{K})}{\alpha + M\phi + L\psi}$$

$$g_L = \frac{bML\psi}{(\alpha + M\phi + L\psi)^2} - \frac{bM}{\alpha + M\phi + L\psi} + \delta\lambda$$

$$g_M = \frac{bML\phi}{(\alpha + M\phi + L\psi)^2} - \frac{bL}{\alpha + M\phi + L\psi}$$

We proceed to evaluate the stability of the semi-trivial equilibria through the Routh-Herwitz criteria, substituting L = 0 and then considering stability at M_1 and M_2:

$$J_{L=0} = \begin{bmatrix} \frac{Mbr}{\alpha + M\phi} - \delta & 0 \\ -\frac{Mb}{\alpha + M\phi} + \delta\lambda & 0 \end{bmatrix}$$

The determinant is zero, so the trace determines stability. We require:

$$\frac{Mbr}{\alpha + M\phi} - \delta < 0$$

Substituting M_1:

$$\frac{rb}{\alpha \cdot \frac{b - \lambda\delta\phi}{\lambda\delta\alpha} + \phi} - \delta < 0$$

$$\Rightarrow \frac{rb\lambda\delta}{b} < \delta \Rightarrow \lambda r < 1$$

Thus, $M_1 < M_2$ is the condition for stability of the semi-trivial equilibrium at M_1 and lower.
For M_2:

$$-\delta + \frac{rb}{\alpha \cdot \frac{rb - \delta\phi}{\delta\alpha} + \phi} < 0$$

$$\Rightarrow -\delta + \frac{rb\delta}{rb} = 0 < 0 \quad \text{(Contradiction)}$$

Hence, M_2 is always an unstable saddle.
Our result for M_1 combined with our graphical analysis suggests the non-trivial steady state will be stable for $\lambda r > 1$, which we will prove algebraically through the Routh-Herwitz criteria.

Theorem 1. *The non-trivial steady state of the system is locally asymptotically stable if and only if* $\lambda r > 1$.

Proof. *We observe:*

$$f_M > 0, \quad g_M < 0 \quad \textit{for all } (M, L)$$

Thus, stability requires:

$$f_L < 0, \quad g_L > 0$$

We proceed to evaluate the remaining Jacobian elements at the non-trivial steady state (M^*, L^*).

1. Sign of g_L***:***

$$\begin{aligned} g_L &= \frac{bM^*L^*\psi}{(\alpha + M^*\phi + L^*\psi)^2} - \frac{bM^*}{\alpha + M^*\phi + L^*\psi} + \delta\lambda \\ &= \delta\lambda - \frac{bM^*(\alpha + \phi M^*)}{(\alpha + M^*\phi + L^*\psi)^2} \end{aligned}$$

From the mineral ODE:

$$\lambda\delta = \frac{bM^*}{\alpha + M^*\phi + L^*\psi}$$

Substituting:

$$g_L = \frac{bM^*}{\alpha + M^*\phi + L^*\psi} \cdot \left(\frac{\psi L^*}{\alpha + M^*\phi + L^*\psi} \right) > 0$$

2. Sign of f_L***:***

$$\begin{aligned} f_L &= -\frac{rbM^*L^*\psi(1 - \frac{L^*}{K})}{(\alpha + M^*\phi + L^*\psi)^2} + \frac{rbM^*(1 - \frac{L^*}{K})}{\alpha + M^*\phi + L^*\psi} - \delta - \frac{rbM^*L^*}{K(\alpha + M^*\phi + L^*\psi)} \\ &= \frac{rbM^*(\alpha + \phi M^*)(1 - \frac{L^*}{K})}{(\alpha + M^*\phi + L^*\psi)^2} - \delta - \frac{rbM^*L^*}{K(\alpha + M^*\phi + L^*\psi)} \end{aligned}$$

Using:

$$L^* = \frac{K}{r}\left(r - \frac{1}{\lambda}\right)$$

We get:

$$f_L = \frac{rbM^*(\alpha + \phi M^*)}{(\alpha + M^*\phi + L^*\psi)^2} \cdot \frac{1}{r\lambda} - \frac{bM^*(r - \frac{1}{\lambda})}{\alpha + M^*\phi + L^*\psi} - \delta$$

Since:

$$-\delta = -\frac{1}{\lambda} \cdot \frac{bM^*}{\alpha + M^*\phi + L^*\psi}$$

We simplify:

$$\begin{aligned} f_L &= \frac{rbM^*}{\alpha + M^*\phi + L^*\psi}\left(\frac{\alpha + \phi M^*}{\alpha + M^*\phi + L^*\psi} \cdot \frac{1}{r\lambda} - 1 \right) \\ &= \frac{rbM^*}{\alpha + \phi M^* + \psi L^*}\left(-\left(1 - \frac{1}{r\lambda}\right) - \frac{\psi L^*}{\alpha + \phi M^* + \psi L^*} \cdot \frac{1}{r\lambda} \right) \end{aligned}$$

Thus:

$$f_L < 0 \quad \textit{if } r\lambda > 1$$

Therefore: *If and only if* $r\lambda > 1$, *we have:*

$$f_M > 0, \quad f_L < 0, \quad g_M < 0, \quad g_L > 0$$

Hence, the Jacobian has negative trace and positive determinant, implying local asymptotic stability of the non-trivial steady state. □

3.5 Biological Interpretation

We observed that the stability of system (1) depends on the balance between remineralisation and plant biomass conversion. When the remineralisation rate, λ, is sufficiently large relative to the biomass conversion rate r, ($r\lambda > 1$), the system reaches a stable, non-trivial equilibrium. This suggests that sufficiently efficient nutrient recycling ensures a continuous supply of minerals for plant growth, supporting a self-sustaining ecosystem. On the other hand, if remineralisation is too slow compared to plant growth ($r\lambda < 1$), the system becomes unstable, leading to nutrient depletion and thus a collapse in plant populations. Therefore, for the ecosystem to remain stable, biomass conversion must result in a self-sustaining model.

4 Plants and Minerals Model with Upwelling Component

4.1 Method of Model Construction

To incorporate artificial upwelling into the Mineral-Plant system, we adapt the model to allow for external nutrient input and associated outflow, transforming the previously closed system into an open one. Upwelling is assumed to deliver nutrients from deeper layers to the surface, increasing the internal mineral concentration. Unless otherwise stated, the assumptions of the original model are retained. Table 2 contains changes made to existing assumptions whilst Table 3 contains new assumptions associated with the impact of AU.

Assumption	**Assumption Type**	**Strength**	**Model Implication**	**Notes / Clarification**
Open system	Dynamical	Strong	External mineral input and loss terms included	Replaces closed system assumption
Upwelling dominates inflow	Biogeochemical	Strong	No other inflow terms	Other mineral inflow is small in scale compared to upwelling
Mineral loss through outflow	Dynamical	Moderate	Maintains volume balance in open system	Prevents unrealistic unbounded increase in mineral concentration

Table 2: Modified current assumptions resulting from Artificial Upwelling

Assumption	Assumption Type	Strength	Model Implication	Notes / Clarification
Time and location chosen to maximise upwelling effectiveness	Spatial / Temporal	Strong	Justifies constant rate and no seasonal variation	Reflects idealised artificial upwelling scenario
Upwelling is constant and uniform	External	Strong	Allows simplification of input term as time-independent	Assumes mechanically forced or engineered upwelling
No impact of upwelling on other parameters	Dynamical	Strong	No feedbacks on plant growth or death rates	Isolates the effect of nutrient supply
No mixing or stratification dynamics	Spatial	Strong	Assumes sharp boundary between layers	Ignores mixed-layer depth effects
Unlimited nutrient availability below	External	Moderate	Ensures constant supply to upper layer	Lower layer treated as infinite reservoir of Minerals

Table 3: New assumptions introduced to model artificial upwelling

Formulating these assumptions results in the following modified system of equations:

$$\frac{dL}{dt} = \frac{rbML}{\alpha + \phi M + \psi L}\left(1 - \frac{L}{K(M)}\right) - \delta L, \tag{3a}$$

$$\frac{dM}{dt} = \lambda\delta L - \frac{bML}{\alpha + \phi M + \psi L} + U - vM, \tag{3b}$$

Where:

U: Nutrient input rate from AU.

v: Outflow/sinking rate of minerals from the upper layer.

We visualise the change to an open system through a box model. We consider the outflow to contribute to the 'infinite' pool of minerals:

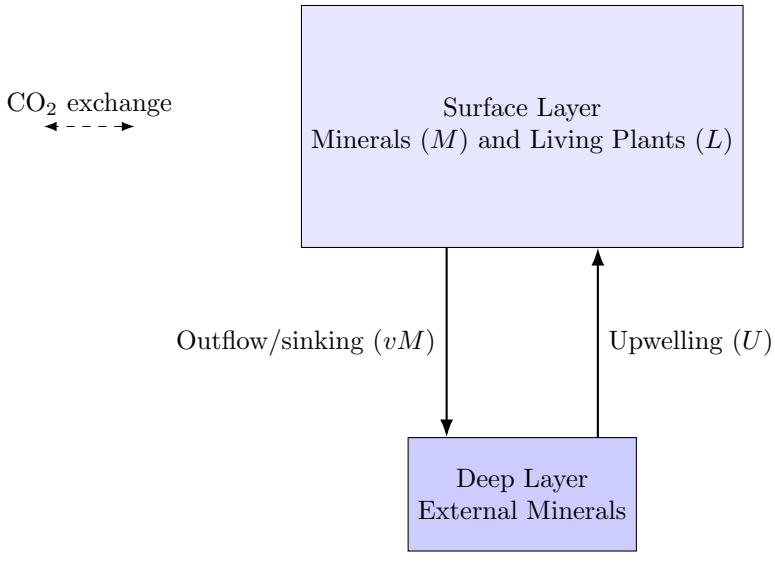

Figure 6: Box model visualising Artifiical Upwelling with no mixed layer

System (3), illustrated in Figure 6, incorporates artificial upwelling through a constant input independent of current mineral levels, representing an increase in mineral concentration to the surface layer. To balance this, we include an outflow term representing the rate at which nutrients are removed, either through sinking or mixing with the surrounding environment. This is essential not only to reflect the physical movement of material but to ensure the system remains bounded and realistic. Without a loss term, nutrients would accumulate indefinitely, leading to unphysical behaviour and distortions in ecosystem dynamics. Including outflow maintains volume and mass balance, accurately capturing the physical behaviour of biomass concentration. This ensures that nutrient cycling remains plausible and that artificial upwelling can be evaluated in a meaningful and interpretable way within the model.

4.2 Graphical Analysis

We illustrate the stability properties of system (3) using phase plane portraits, providing a visual insight into the dynamics introduced by artificial upwelling. The inclusion of the constant upwelling term U fundamentally alters the system's behaviour. Previously, the model admitted a line of stability along $L = 0$. This is eliminated by including U, which sustains a nonzero mineral input and results in a semi-trivial intercept. The addition of U also increases the complexity of the system: both nullclines now exhibit parabolic structure, which introduces the potential for multiple interior equilibria. By varying the magnitude of U, we observe three qualitatively distinct scenarios, corresponding to the emergence of one, two, or three equilibrium points. We note that the model stabalises for sufficently small α, resulting in similar stability dynamics regardless of U.

The phase plane portraits below are constructed using the following example parameter values: $K = 5$, $r = 4$, $b = 1.5$, $\phi = 0.2$, $\psi = 0.1$, $\delta = 1.2$, $\lambda = 1$, and $v = 1.5$. Figures 7, 8, and 9 correspond to upwelling rates $U = 0.1$, $U = 0.5$, and $U = 1.5$, respectively with $\alpha = 3$, illustrating how U acts as a bifurcation parameter when the half saturation rate is large. Figure 10 shows a state where alpha is small so the bifurcating effect of U is limited

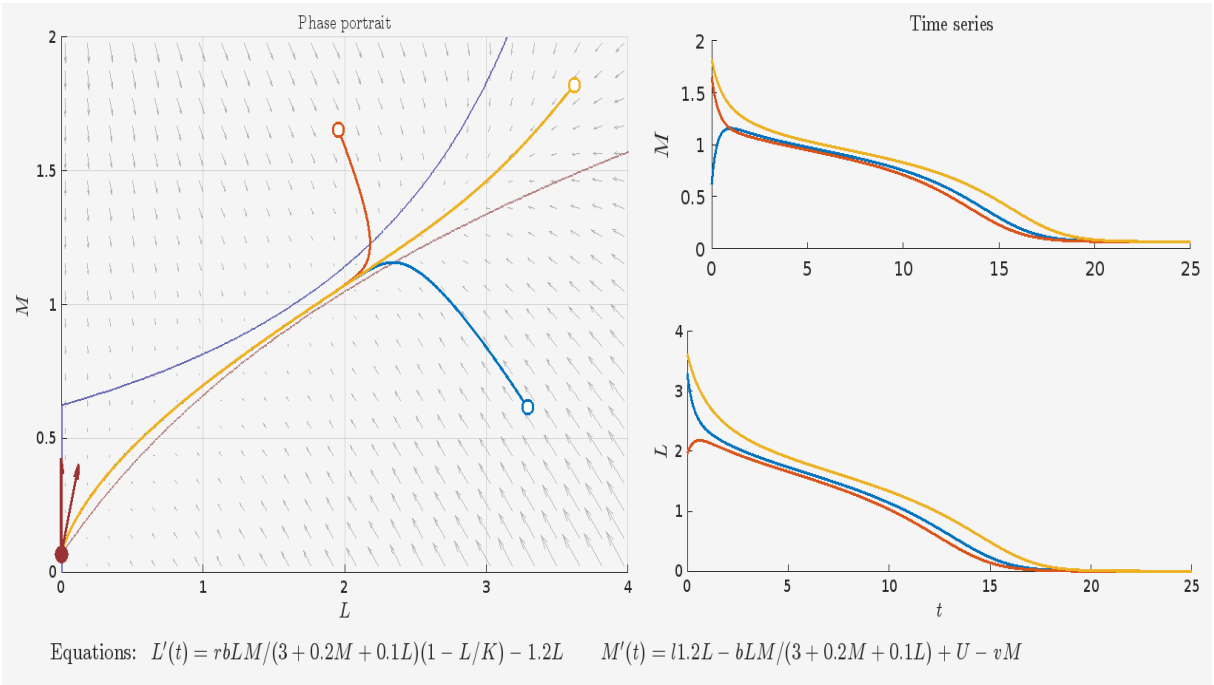

Figure 7: Mineral-Plant Model with upwelling, 1 steady state, α large

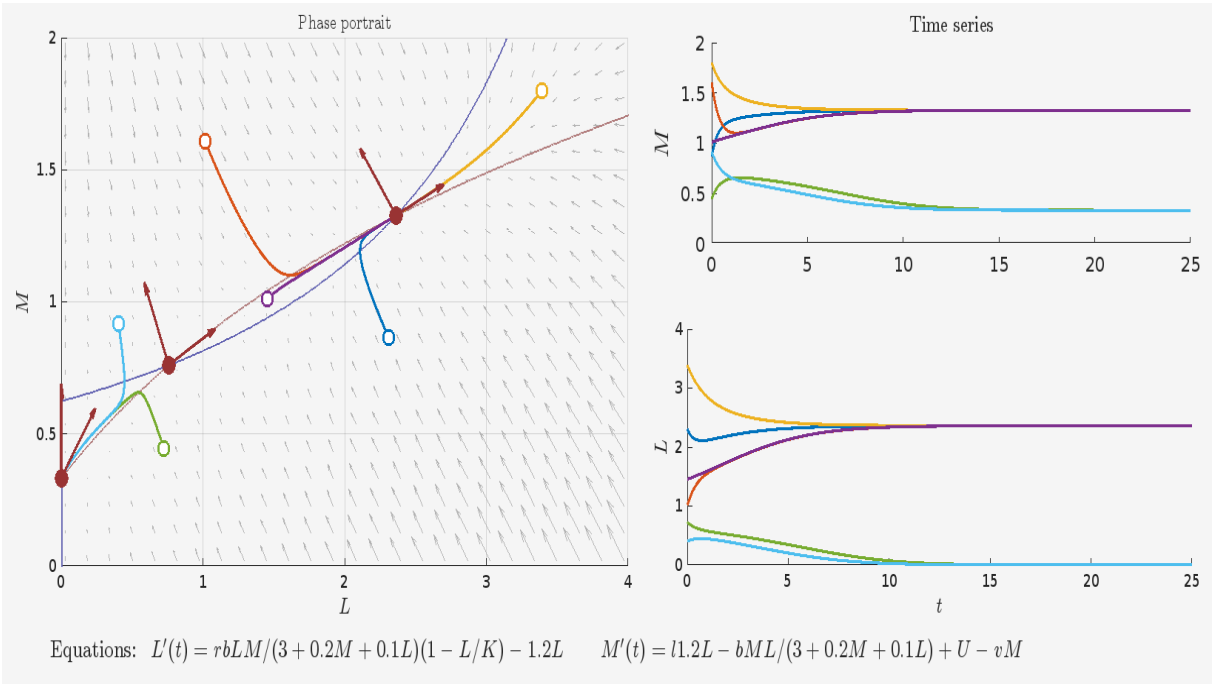

Figure 8: Mineral-Plant Model with upwelling, 3 steady states, α large

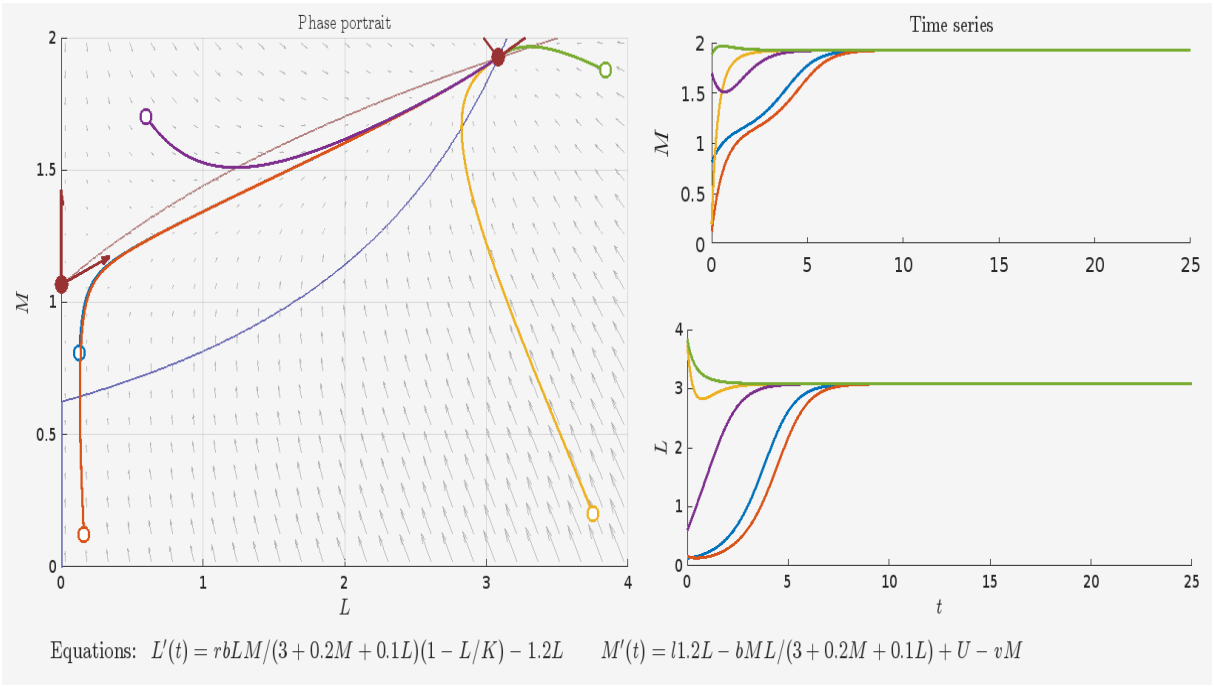

Figure 9: Mineral-Plant Model with upwelling, 2 steady states, α large

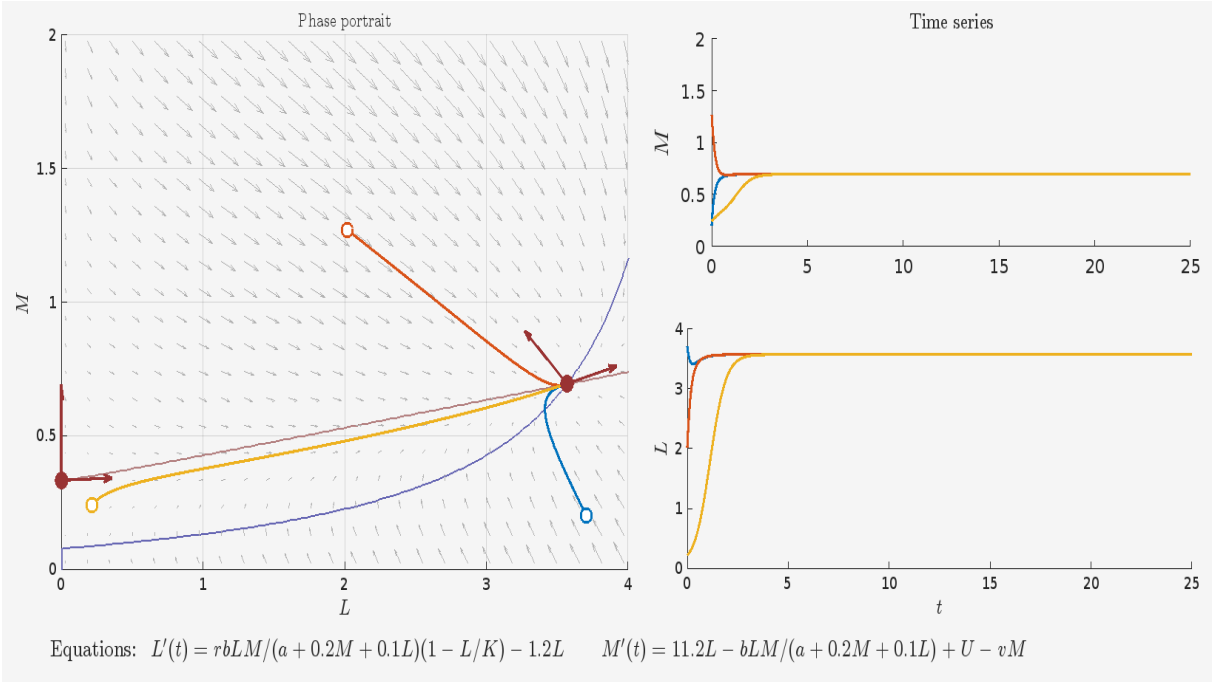

Figure 10: Mineral-Plant Model with upwelling, 2 steady states,α small

For larger values of α, we see nutrient uptake becomes more efficient at low mineral concentrations, resulting in a system that is highly sensitive to the upwelling rate U. In this case, changes in U can lead to significant qualitative shifts in the number and stability of equilibria, as shown in Figures 7-9. However, when α is sufficiently small, uptake is inefficient unless mineral concentrations are high, flattening the mineral nullcline until it curves away from the the L-axis. This limits its intersections with the plant nullcline.

As demonstrated in Figure 10, this causes the system to stabilise at a single, non-trivial equilibrium for all U, bar extremely small values (< 0.1). The semi-trivial equilibrium remains unstable throughout, indicating that in nutrient-limited environments with low half-saturation thresholds, external nutrient forcing has diminished influence on the overall ecosystem dynamics.

In the case of larger alpha, we see as U increases, we see the emergence of a stable non-trivial equilibrium, resulting in bi-stability until the semi-trivial equilibrium switches. Once U exceeds a critical threshold ($U \approx 1.27$ for the given parameters), the equilibrium becomes unstable and the number of equilibria reduces from three to two, indicating a transcritical bifurcation. The model remains in this state as U increases. Although this bifurcation is clearly reflected in the behaviour of the semi-trivial equilibrium, the point at which the two interior equilibria first emerge is not directly associated with any stability change in the semi-trivial case, suggesting the non-trivial equilibria obey a more nuanced underlying behaviour. We seek to quantify the changes in semi-trivial and non-trivial stability through studying the Jacobian of the system at different equilibria.

4.3 Algebraic Analysis

We note that stability in this extended model is more intricate than in the closed system, relying not only on biomass conversion rates r and λ, but also production and per capita mortality rates b and δ, and most predominantly, the upwelling terms U and v. The introduction of external nutrient input alters both the structure and interpretation of the steady states. In particular, the non-trivial nullclines now form quadratics, increasing the algebraic complexity and reducing our ability to determine specific analytical solutions. Moreover, the non-trivial steady states no longer share the same qualitative properties as in the closed system, so similar conclusions relating r and λ cannot be made without

further analysis.

Semi-Trivial Steady State

We identify a semi-trivial steady state where the mineral nullcline intersects the M-axis. Substituting $L = 0$ we obtain the following:

$$M_5 = \frac{U}{v},$$

such that $(M_5, 0)$ is a steady state of the system.

Stability Analysis

We compute the Jacobian matrix of the system:

$$f_L = \frac{-K\delta(\alpha + M\phi + L\psi)^2 - LMb\psi r(K - L) + Mrb(K - 2L)(\alpha + M\phi + L\psi)}{K(\alpha + M\phi + L\psi)^2}$$

$$f_M = \frac{Lbr(K - L)(L\psi + \alpha)}{K(\alpha + M\phi + L\psi)^2}$$

$$g_L = -\frac{M^2 b\phi + M\alpha b}{(\alpha + M\phi + L\psi)^2} + \delta\lambda$$

$$g_M = -\frac{L^2 b\psi + L\alpha b}{(\alpha + M\phi + L\psi)^2} - v$$

As in the model without upwelling, we observe $f_M > 0$ and $g_M < 0$, thus at the semi-trivial steady state $(M_5, 0)$, the Jacobian simplifies to:

$$J = \begin{bmatrix} f_L = \dfrac{-\delta(\alpha + M_5\phi)^2 + M_5 rb(\alpha + M_5\phi)}{(\alpha + M_5\phi)^2} & 0 \\ g_L = -\dfrac{M_5^2 b\phi + M_5\alpha b}{(\alpha + M_5\phi)^2} + \delta\lambda & -v \end{bmatrix}$$

Since this Jacobian is upper triangular, the eigenvalues are therefore the diagonal entries: f_L and $g_M = -v < 0$. Therefore, stability is determined by the sign of f_L, which gives the following condition for stability of the semi-trivial nullcline.

$$\frac{U}{v}(rb - \delta\phi) < \delta\alpha$$

This condition explains the contrast between the behaviours seen in Figures 7-9 and Figure 10. When α is small, the right-hand side of the inequality is also small, making the condition more difficult to satisfy. This means that the inequality is more likely to be violated, leading to an unstable semi-trivial equilibrium regardless of the upwelling rate U. In contrast, for larger values of α, the inequality can hold for a range of U, allowing for a change in the stability of the semi-trivial equilibrium as U increases. This aligns with the observation that stability varies with U when α is large, but remains fixed when α is small.

Non-Trivial Steady States

The non-trivial steady states arise from solving a quadratic system, which render much less interpretable results when solved. Nonetheless, we observe from the phase portraits that for sufficiently large alpha, as U increases the number and nature of steady states change. These transitions are best captured through bifurcation diagrams, where U is treated as a bifurcation parameter.

4.4 Bifurcation Analysis

We visualise the change in stability as U increases relative to both state variables, L and M. Current parameter values have been maintained.

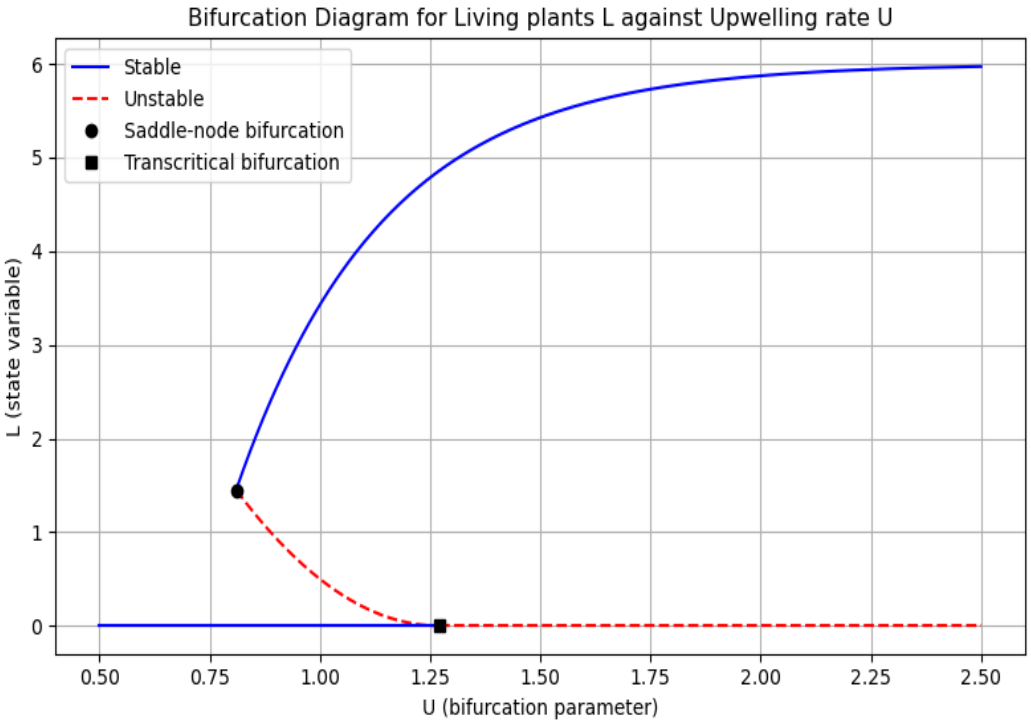

Figure 11: Bifurcation of upwelling rate U with respect to plant density L

Note that for Figure 11, the stable upper branch eventually reaches carrying capacity for large U, however the diagram shows it at a smaller value for the sake of illustrating the overall dynamics.

The bifurcation diagrams visualise how the stability of the system changes for the chosen example values (sufficiently large α) whilst increasing upwelling rate U relative to the density of living plants (equivalent results can be seen relative to mineral concentration M). As U increases, the mineral concentration M increases, and the semi-trivial steady state remains stable. When U becomes sufficiently large, the non-trivial equilibrium becomes feasible. This results in a saddle node bifurcation which separates the non-trivial nullclines into a stable upper branch and an unstable lower branch, for a total of 3 equilibria which demonstrates the bistability noted earlier. As the unstable lower branch exits the positive quadrant, the stability of the semi-trivial equilibrium transitions from stable to unstable resulting in a transcritical bifurcation.

4.5 Biological Interpretation

We see that as the upwelling rate increases, the system tends toward a stable plant population regardless of initial conditions, provided there is a non-zero initial mineral concentration. This reflects a scenario in which a sustained external input of nutrients (via upwelling) counteracts the mineral loss from sinking, enabling long-term plant survival and growth. Thus even if the initial plant biomass is low, the continual nutrient input eventually supports the conditions needed for population recovery. While this is a simplified representation chosen at an optimal time point for upwelling (the parameters in the model would vary over time) it still captures a core ecological mechanism: when nutrients are reliably supplied, autotrophic populations are more likely to stabilise and persist over time.

While this model offers insight into how upwelling influences plant-mineral dynamics, the algebraic complexity limits our analytical understanding of the model which in turn limits biological interpretation. Biologically, artificial upwelling is most commonly employed to stimulate phytoplankton growth in marine environments with nutrient and light are the primary limiting factors. This motivates a shift toward refining the model within a NP framework, which more accurately reflects the ecosystems where artificial upwelling is typically applied. A refined model would allow for less assumptions which limit interpretability, resulting in a model simple enough to support the introduction of seasonality. This balance between biological realism and mathematical limitation is essential for understanding the long-term effects of upwelling interventions in open marine systems.

5 Refined Model for Nutrient-Phytoplankton Dynamics

5.1 Refined Assumptions

To create a refined model for AU, we first modify the previous assumptions to coincide with Nutrient-Plankton dynamics.

Research shows that many phytoplankton models do not incorporate limiting factors such as carrying capacity K or saturation rate ψ, due to the implicit assumption of abundant spatial resources in open ocean systems [19]. Instead, light and nutrients are the primary limiting factors influencing growth, particularly in oligotrophic condition where AU interventions are most effectively applied. This motivates the development of a simpler model that better captures these dynamics.

Traditional NPZ models such as those discussed by Narwani et al. [4] and detailed in the comprehensive review by Franks [27] introduce additional complexity, including zooplankton grazing and detrital compartments. Whilst we simplify our dynamics to exclude these compartments, the structures discussed in Franks [27] can be applied to NP models. This establishes a precedent for our model components, such as a direct link between phytoplankton death and remineralisation, the incorporation of Michaelis-Menten effects, as well as dropping a phytoplankton carrying capacity. Whilst this review primarily discusses closed systems, the dynamics are seen in open models too.

Specifically, Jajeh [28] sets a precedent for incorporating these effects in open systems where nutrient forcing plays a dominant role in shaping bloom outcomes. To incorporate upwelling in this context, we include a constant net exchange term E representing a continuous input/output of nutrients from/to deeper waters, independent of the current nutrient concentration. While this assumption departs from biological realism, since loss terms are generally proportional to nutrient levels, as shown in Jajeh [28], it allows for a simpler and more adaptable model.

Additionally, we assume the system evolves over a longer temporal scale (e.g., yearly), to reflect the seasonal development and decline of phytoplankton blooms when seasonality is introduced.

5.2 NP Model Equations

The proposed model equations are as follows:

$$\frac{dP}{dt} = \frac{rbNP}{\alpha + \phi N} - \delta P \tag{4a}$$

$$\frac{dN}{dt} = \lambda\delta P - \frac{bNP}{\alpha + \phi N} + E \tag{4b}$$

where:

- P is phytoplankton biomass (mmol m^{-3}),
- N is nutrient concentration (mmol m^{-3}),

- E is the net external nutrient input rate from upwelling (mmol m^{-3}),
- t is time ([t])
- b is the maximum uptake rate ($[t]^{-1}$),
- r is the biomass conversion efficiency (dimensionless),
- α is the half-saturation constant for nutrient uptake (mmol m^{-3}),
- ϕ is a scaling parameter adjusting nutrient uptake saturation (dimensionless),
- δ is the per capita phytoplankton mortality rate ($[t]^{-1}$),
- λ is the fraction of biomass that is remineralised to nutrients upon death (dimensionless).

Note that E, the net nutrient exchange rate, can be negative as well as positive, demonstrating an overall loss in nutrients. This refined model captures key ecological processes in a simplified, analysable framework and provides a foundation for future incorporation of seasonal dynamics and grazing effects.

5.3 Graphical Analysis

We perform graphical analysis to visualise how the stability of system (4) changes for different parameter values. The phase plane portraits are generated using the following example parameter values: ,$b = 3$, $\alpha = 0.3$, $\phi = 0.4$, $\delta = 1$, and $\lambda = 0.5$. We consider 4 different cases, $E = 0.5, r = 0.4$, $E = -0.5, r = 0.5$, $E = 0.5, r = 3$ and $E = -0.5, r = 3$.

When the parameters are modified to $E = -0.5$ and $r = 3$, varying the sign of the net exchange term E changes model dynamics, allowing nutrients to either overall increase or decrease, depending on whether the system is self sustaining or not. We see the nullclines tending away from the origin for positive exchange rate and towards the origin when negative. This in turn requires the linear phytoplankton nullcline to intersect at higher or lower values of N to produce an equilibrium.

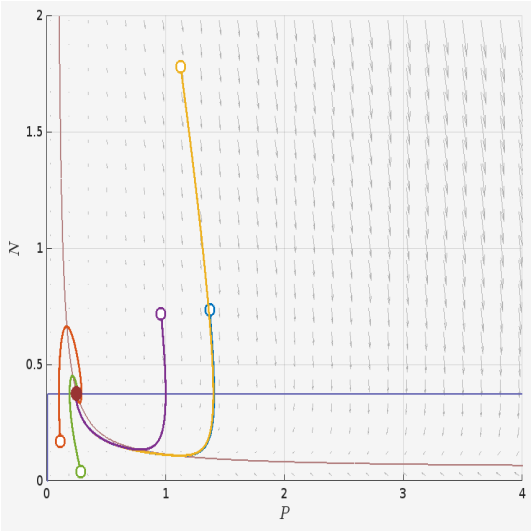

Figure 12: NP model with E = 0.5, r = 0.4

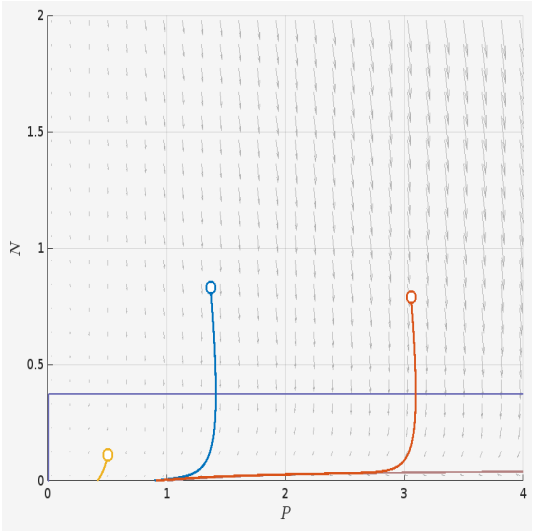

Figure 13: NP model with E = -0.5, r = 0.4

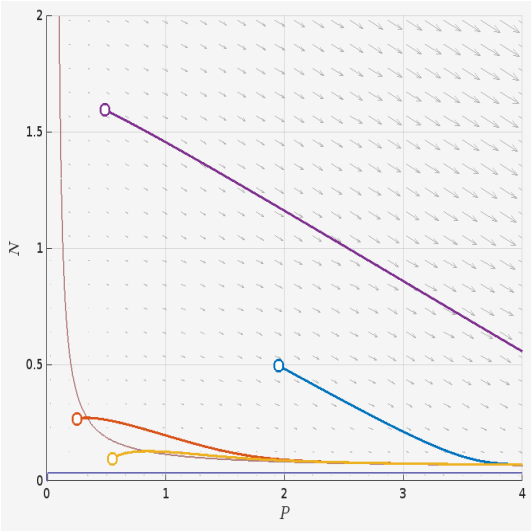

Figure 14: NP model with E = 0.5, r = 3

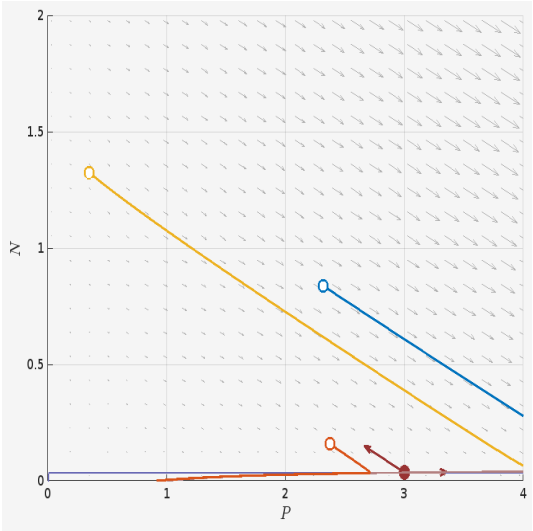

Figure 15: NP model with E = -0.5, r = 3

We observe the emergence of an equilibrium whose nature depends on the values of r and E. In particular, when $E > 0$ and r is sufficiently small, the system exhibits a spiral sink, indicating damped oscillations around a stable steady state. This behaviour mirrors findings in the current literature, notably in Kovac [18], where system stability was shown to depend on the balance between biomass loss and nutrient supply. These observations imply that oscillations are a likely feature of spring blooms, when biomass conversion efficiency is low.

The sensitivity of stability to the biomass conversion rate r further suggests that, as in the closed Mineral-Plant model, the basic NP model's dynamics are governed by $(r\lambda\ )$, in addition to E. To explore this relationship precisely, we compute the Jacobian matrix at the non-trivial steady state.

5.4 Algebraic Analysis

Given there is only one or no equilibrium at a non-trivial steady state, we obtain the following non-trivial equilibrium for system (4): 2

$$N^* = \frac{\alpha\delta}{rb - \phi\delta}$$

$$P^* = \frac{E}{\dfrac{bN^*}{\alpha + \phi N^*} - \lambda\delta}$$

We compute the Jacobian matrix for system (4) evaluated at the non-trivial steady state (P^*, N^*), obtaining:

$$J = \begin{bmatrix} 0 & \dfrac{E(br - \delta\phi)^2}{\alpha b\delta(1 - \lambda r)} \\ \delta r(\lambda r - 1) & \dfrac{E(br - \delta\phi)^2}{\alpha b\delta r(\lambda r - 1)} \end{bmatrix}$$

To determine the stability of the steady state, we apply the Routh-Hurwitz criteria, and note that the Jacobian entries depend on the sign of $\lambda r - 1$ and E:

- For $E > 0$:
  - If $\lambda r > 1$, then both off-diagonal terms are positive, and Trace$(J) > 0$, Det$(J) > 0$ corresponding to an unstable spiral.
  - If $\lambda r < 1$, then the signs flip: Trace$(J) < 0$, Det$(J) > 0$ resulting in a spiral sink.

However, graphical analysis indicates that parameter combinations with $\lambda r > 1$ and $E > 0$ do not yield a real non-trivial equilibrium, so only the stable spiral is observed.

- For $E < 0$:
  - If $\lambda r < 1$, then the denominator of the Jacobian entries becomes singular or negative, and no real steady state exists.
  - If $\lambda r > 1$, then the trace is positive and determinant is positive producing an unstable spiral.

Thus, the system exhibits a spiral sink only when $E > 0$ and $\lambda r < 1$, consistent with conditions representing low biomass conversion during spring bloom periods.

5.5 Introducing Artificial Upwelling

In this model, we assume the effect of artificial upwelling increases the net exchange in nutrient concentration, implying that for systems with sufficiently small biomass conversion rate, stability can be forced through AU. This a similar result to the Mineral-Plant Model with Upwelling, where increasing the upwelling rate leads to model stability.

5.6 Comparing Mineral-Plant Model to Nutrient-Plankton Model

We note that the $r\lambda$ condition for stability observed in the Mineral-Plant model is also observed in the NP model, however it is inverted, with stability only occuring when $r\lambda < 1$.
A key distinction between the Mineral-Plant model and the NP-model lies in the nature of the saturation term governing growth. In the Mineral-Plant model, crowding effects are explicitly included via a saturation function of the form $\alpha + \phi N + \psi P$, which accounts for both nutrient limitation and density-dependent constraints. In contrast, the NP model omits the plant/phytoplankton dependent term, using $\alpha + \phi N$ instead, i.e. assuming that such crowding effects are negligible. This difference has notable implications for the model's stability behaviour.

In the Mineral-Plant model, stability is observed when $\lambda r > 1$, meaning that a high remineralisation-to-conversion ratio is required for the model to be self-sustaining. Conversely, the NP model which lacks crowding feedbacks, is stable only when $\lambda r < 1$. Here, the absence of self-limitation means the system only remains stable if conversion is sufficiently weak relative to remineralisation. In addition, the inclusion of the exchange term E continuously increases the nutrient concentration of the model, which will increase unboundedly in the NP model if $r\lambda > 1$.

This reversal highlights that the parameter relationship λr has different interpretations depending on ecological context: in scenarios such as Nutrient-Phytoplankton dynamics where we expect a bloom , the NP model is more appropriate, demonstrating oscillatory dynamics and the runaway effect at the beginning of a bloom, while in systems where crowding effects take place, $r\lambda$ must be higher for the system to be self-sustaining and reach an equilibrium.

Thus the stability conditions observed in the NP model reflect biological dependencies necessary to model seasonal phytoplankton blooms, which we proceed to model.

6 Introducing Seasonality

In the following section, we introduce seasonality to model phytoplankton blooms. Current literature, such as [19], employs changes in mixed layer depth to trigger blooms. During phytoplankton blooms, stratification tends to weaken, leading to a deeper mixed layer (note that in this model this considered to be an upper layer with no stratification in the mixing, and a hard boundary between upper and lower layers). This process enhances nutrient availability, which in turn stimulates the bloom. The

literature review an increase in zooplankton predation during spring blooms, but not during autumn blooms. This suggests that autumn blooms would be more appropriate for our model, given that we exclude zooplankton. However, post-autumn bloom growth conditions are generally poor, whereas light and temperature are more favourable during summer months. Therefore, we focus on modelling upwelling after the spring bloom and address potential concerns associated with omitting zooplankton in our analysis.

We approach the induction of blooms through stratification from two perspectives. First, a top-down approach is used, where a wave function is applied to the remineralisation rate. This reflects how an expanding upper eutrophic layer increases the proportion of nutrients that are reintroduced into the model before they sink. Additionally, we explore a bottom-up approach to model oscillations internally, avoiding the introduction of time-dependent variables that would complicate the analysis of the system.

6.1 Top-down Approach

We modify system (4) by adjusting the remineralisation term, $\lambda(t)$, as follows:

$$\lambda(t) = \bar{\lambda}\left(1 - 0.4\cos\left(\frac{2\pi(t-38)}{52}\right)\right)$$

Here, $\bar{\lambda}$ represents the median value of λ, while the factor 0.4 determines the magnitude of the oscillations. The argument of the cosine function governs the timing of the bloom die-off, with the periodicity set to 52 weeks, corresponding to the annual cycle.

Using the following example parameter values: $r = 1.2$, $b = 1.6$, $\delta = 1$, $\alpha = 0.5$, $\phi = 1$, $\bar{\lambda} = 0.3$, and $E = 1$, we obtain the resulting time series for nutrient and phytoplankton concentrations as shown below.

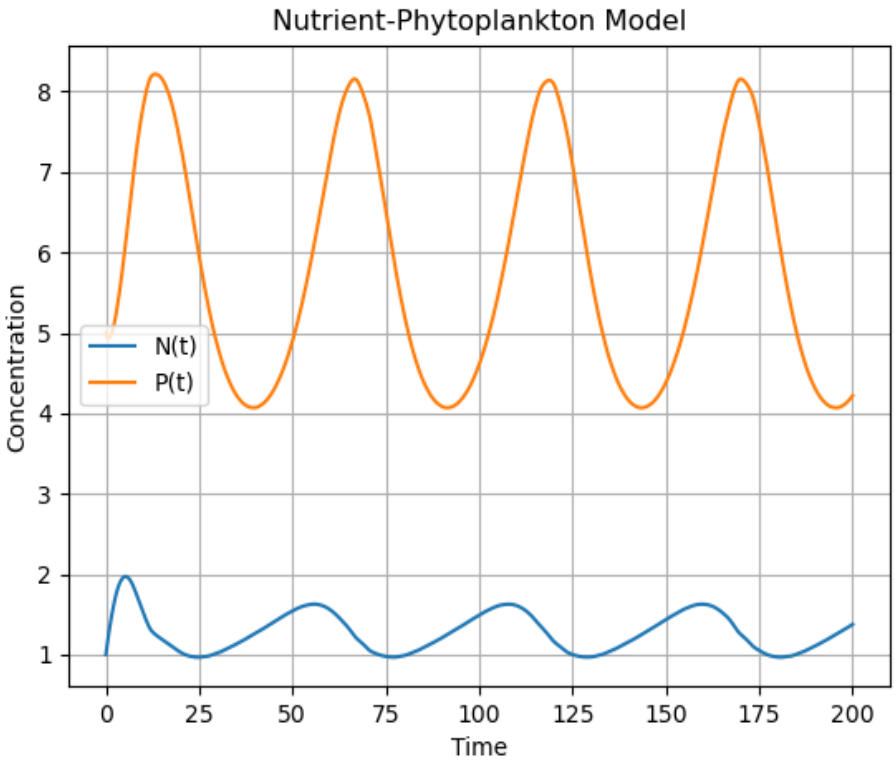

Figure 16: Top-down forced oscillations over 200 weeks

Given that λ is chosen to be at most $0.3 * 1.4$ given the values in the wave function defined above, in Figure 16 we have that the system remains stable according to our stability analysis of system (4). An increase in $\bar{\lambda}$ results in $r\lambda > 1$, which results in instability, however modifying the remineralisation term through a wave function, this results in unrealistic solutions (negative nutrient concentration).

6.2 Bottom-up Approach

To capture internally generated oscillations without explicitly introducing time-dependent forcing, we modify the nutrient-phytoplankton model to include a feedback mechanism driven by net nutrient exchange. This approach assumes that as stratification weakens (e.g. due to seasonal dynamics), the upper layer deepens, allowing more nutrient-rich water to enter the euphotic zone. As a result, nutrient availability increases, stimulating phytoplankton growth, which in turn increases uptake to mirror the deepening of the upper layer.

This feedback loop allows the system to exhibit self-sustained oscillations, but is not a completely accurate reflection of dynamics due to an inversion of causality. In reality, it is the physical deepening of the mixed layer-driven by external seasonal effects such as temperature and increased density gradients that increases nutrient entrainment, rather than higher nutrient concentrations triggering enhanced inflow. As such, the model captures the emergent behaviour of blooms and crashes, but does so by reversing the causal relationship between mixing and nutrient availability. Despite this simplification, the approach offers a useful proxy for studying bloom dynamics in the absence of explicit environmental forcing.

We represent this by introducing non-linear inflow and outflow terms into the nutrient equation, leading to the following system:

$$\frac{dP}{dt} = \frac{rbNP}{\alpha + \phi N} - \delta P \tag{5a}$$

$$\frac{dN}{dt} = \lambda\delta P - \frac{bNP}{\alpha + \phi N} + \frac{IN}{N + K} \tag{5b}$$

The net inflow term $\frac{IN}{N+K}$ captures the saturating nature of nutrient entrainment due to stratification: when nutrient levels are low, inflow is limited, but as N increases, it enhances nutrient entrainment up to a maximum controlled by I, the intrinsic inflow rate. The parameter K serves as a proxy for the critical depth (as per Sverdrup's critical depth hypothesis [21]), which marks the threshold beyond which phytoplankton growth is no longer sustainable due to insufficient light. While this simplification assumes a constant growth rate and a sharp light cut-off, it provides a useful approximation of the effect of vertical stratification.

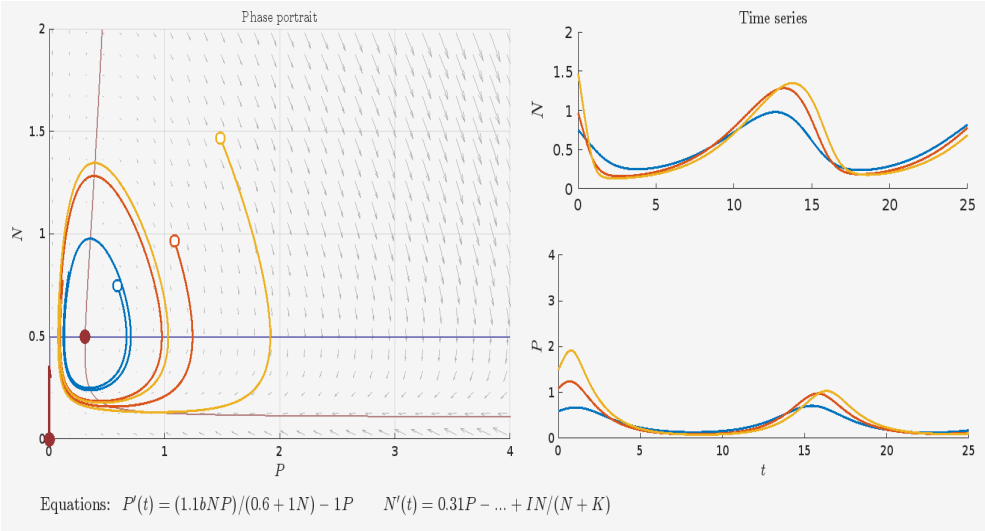

Figure 17: Phase portrait of the nutrient-phytoplankton model with nutrient inflow and outflow indicating internally driven oscillations

The above model was constructed using the following example parameter values, chosen to induce oscillatory behaviour:

$$b = 2, \quad I = 2.1, \quad K = 4, \quad r = 1.1, \quad \alpha = 0.6, \quad \phi = 1, \quad \delta = 1, \quad \lambda = 0.3.$$

The emergence of oscillations in this model aligns with qualitative expectations of phytoplankton bloom cycles. However, the amplitude and frequency of these oscillations are highly sensitive to parameter choices, which may not correspond directly to biological or environmental variability observed in nature. This sensitivity highlights a limitation in the model's realism, as small perturbations in certain parameters can lead to disproportionately large changes in system behaviour. Nonetheless, the ability of the model to internally generate bloom-like dynamics-without explicit time-dependent forcing-demonstrates its potential as a minimal framework for capturing seasonal behaviour through intrinsic feedback mechanisms, suggesting adaptations could be used such as reintroducing a dynamic carrying capacity to reflect the change in euphotic layer depth.

6.3 Comparison of Methods

Comparing the bottom-up and top-down approaches, we see each derived model offers distinct advantages. Internally generated oscillations in bottom-up approach are easier to define within the model as they emerge directly from the system's internal feedbacks. However, the reversed causality in this method, where increased nutrient levels supposedly drive upwelling, presents challenges when trying to adapt the model to more realistic dynamics. The top-down method does not suffer from the causality inversion problem, allowing it to be more easily adapted to changing parameters, however introducing upwelling does not currently stabilise the NP model, as seen in the Mineral-Plant model.

In both oscillating systems, we introduce upwelling by modifying the nutrient exchange terms E and I, respectively. While adjusting the net inflow does not directly affect stability which depends on the sign of the Jacobian components, it does amplify the strength of oscillations. Manipulating I and K in the bottom-up system, which governs limit cycles, alters the magnitude of oscillations. However, as previously noted, the model's sensitivity to small perturbations means that these results should be interpreted cautiously. Thus, the framework requires further refinement to accommodate for realistic ecological dynamics.

For future work, reintroducing a dynamic carrying capacity for phytoplankton, explicitly linked to stratification depth, would help avoid unrealistic bloom magnitudes and bring the model more in line

with observed ecological patterns, particularly in the bottom up model. Additionally, incorporating a carbon feedback loop would be valuable. This would involve developing an oscillating model with a carbon sequestration equation to ensure that upwelling does not inadvertently lead to outgassing. Ideally incorporating upwelling into either model would lead to longer more sustained blooms, as the literature suggests, as post-spring bloom conditions are ideal for inducing blooms through artificial upwelling.

7 Conclusions

We see that different modelling approaches offer complementary insights. The plant-mineral model demonstrates stable dynamics, but only within a framework of sustained self-growth (resulting from sufficient biomass conversion rates) constrained by crowding effects and environmental carrying capacity. By contrast, the simplified nutrient-phytoplankton (NP) model is built as an open system and thus more readily adapted to represent artificial upwelling. By relying on a positive net nutrient influx to maintain stability, it produces a spiral sink under low biomass conversion rates, similar to observations in current literature [18]. When biomass conversion rates are sufficiently high, the NP model exhibits unbounded growth, similar to behaviour observed at the beginning of a bloom. This suggests that the model's most realistic application lies when coupling moderate growth with continuous external input to demonstrate conditions characteristic of seasonal deepening of the mixed layer. Modifying nutrient exchange to mimic stratification generates seasonal oscillations, yet such forced limit cycles can be highly sensitive to parameter perturbations, and may struggle to accurately represent dynamics (e.g. reversed causality in the above model).

Introducing time-dependent seasonal terms thorough a wave function may result in an more flexible model, which represents dynamics better, however such a model has its own caveats, such as being oversensitive to changes in stability. This suggests a well framed time-dependent model would offer the best results, however an algebraic comparison of internal versus external mechanisms for inducing seasonality-accompanied by sensitivity analyses-would clarify the necessary conditions for robust oscillatory behaviour and thereby evaluate each approaches suitability for studying artificial upwelling. In the plant-mineral model, previously unstable regimes become stable once upwelling was introduced, thus we expect that in a properly formulated seasonal NP model, upwelling will equivalently prolong blooms.

While we have not explicitly included a carbon term in the model, we assume that carbon sequestration is directly linked to phytoplankton biomass. Under this assumption, upwelling enhances nutrient availability, which in turn promotes phytoplankton growth. Thus we can study how sequestration changes based on the level of phytoplankton mortality in the model, decreasing the remineralisation term. For the Mineral-Plant model we would require stronger upwelling or a stronger biomass conversion rate to ensure stability with a reduced remineralisation rate.

In the NP model, the decrease in remineralisation would result in a more stable model, however this decreases the magnitude of the stability point, realistically representing how less nutrients in the model due to sequestration results in less growth. With additional development, the NP framework could be extended into three dimensions to include carbon dynamics and investigate how sustained or pulsed upwelling influences net carbon export. Such a model could help identify thresholds beyond which excessive upwelling causes outgassing rather than sequestration, and highlight the need for controlled nutrient input.

Using biologically realistic values for the parameters over example values would aid modelling significantly as it would offer crucial insight as to whether upwelling is effective in a realistic scenario.To fur-

ther increase biological realism, incorporating zooplankton grazing would better demonstrate bloom termination phases and help regulate oscillatory behaviour. Similarly, explicitly resolving depth-dependent processes, such as stratified light availability and vertical mixing would allow the model to capture the physical drivers of stratification more accurately. Existing NPZ and NPZD models [4] have successfully demonstrated oscillations through such mechanisms, suggesting that blending these ecological interactions with physically informed upwelling terms could produce more robust, seasonally realistic outcomes. Analysing such models, potentially with the addition of a carbon sequestration equation, would assist in evaluating the applicability of Artificial Upwelling to mitigate climate change.

References

[1] Met Office. (2024). *Forecast for 2025 CO_2 concentration levels.* https://www.metoffice.gov.uk/research/climate/seasonal-to-decadal/long-range/forecasts/co2-forecast-for-2025

[2] National Academies of Sciences, Engineering, and Medicine. (2015). *Climate Intervention: Carbon Dioxide Removal and Reliable Sequestration.* The National Academies Press. https://denverclimatestudygroup.com/wp-content/uploads/2015/04/Climate-Intervention-Carbon-Dioxide-Removal-and-Reliable-Sequestration.pdf

[3] National Center for Biotechnology Information. (2021). *The Ocean Carbon Sink.* https://www.ncbi.nlm.nih.gov/books/NBK580044/

[4] Narwani, A., et al. (2023). NPZD modeling for marine systems. *Journal of Mathematical Biology.* https://link.springer.com/article/10.1007/s00285-023-01969-7

[5] Sverdrup, H. U. (1953). On conditions for the vernal blooming of phytoplankton. https://www.soest.hawaii.edu/oceanography/courses/OCN626/2010/sverdrup.pdf

[6] Macdonald, J. C., & Gulbudak, H. (2023). Forward hysteresis and Hopf bifurcation in an NPZD model with application to harmful algal blooms. *Journal of Mathematical Biology*, 87(3), 45. https://link.springer.com/article/10.1007/s00285-023-01969-7

[7] Wirtz, K. W., & Eckhardt, B. (2006). Effective variables in ecosystem models with an application to phytoplankton succession. *Journal of Plankton Research, 28*(2), 209–221. https://academic.oup.com/plankt/article/28/2/209/1428450

[8] Oschlies, A., & Pahlow, M. (2023). Earth system model projections of artificial upwelling. *Geophysical Research Letters.* https://agupubs.onlinelibrary.wiley.com/doi/10.1029/2022GL101870

[9] Suess, E., et al. (2021). CFD modelling of artificial upwelling. *Frontiers in Marine Science, 8*, 804875. https://www.frontiersin.org/journals/marine-science/articles/10.3389/fmars.2021.804875/full/

[10] Klausmeier, C. A., et al. (2000). Optimality and NP-models in plankton ecology. *Journal of Plankton Research, 22*(9), 1619–1648. https://academic.oup.com/plankt/article-abstract/22/9/1619/1478094

[11] Yoshiyama, K., & Nakajima, H. (2002). Simple NP model under upwelling conditions. *Hydrobiologia, 484*, 189–200. https://link.springer.com/article/10.1023/A%3A1015874028196

[12] National Academies of Sciences, Engineering, and Medicine. (2021). *A Research Strategy for Ocean-based Carbon Dioxide Removal and Sequestration.*

https://www.frontiersin.org/journals/marine-science/articles/10.3389/fmars.2022.841894/full

[13] Oschlies, A., Pahlow, M., Yool, A., & Matear, R. J. (2010). Climate engineering by artificial ocean upwelling: Channelling the sorcerer's apprentice. *Geophysical Research Letters, 37*(4). https://agupubs.onlinelibrary.wiley.com/doi/10.1029/2009GL041961

[14] Pan, X., et al. (2015). Evaluation of the sinks and sources of atmospheric CO_2 by artificial upwelling. *Science of The Total Environment, 512–513*, 492–503. https://www.sciencedirect.com/science/article/pii/S0048969714016544

[15] Jürchott, A., Oschlies, A., & Koeve, W. (2023). Artificial Upwelling-A Refined Narrative. *Geophysical Research Letters, 50*(1). https://agupubs.onlinelibrary.wiley.com/doi/10.1029/2022GL101870

[16] Heinemann, M., et al. (2021). Effect of Intensity and Mode of Artificial Upwelling on Particle Flux and Carbon Export. *Frontiers in Marine Science, 8*, 742142. https://www.frontiersin.org/journals/marine-science/articles/10.3389/fmars.2021.742142/full

[17] Riley, G. A. (1946). Factors controlling phytoplankton populations on Georges Bank. *Journal of Marine Research*, 6(1), 54–73.

[18] Kovac, Z. (2021). Nutrient-phytoplankton interactions in stratified waters: A theoretical perspective. *ICES Journal of Marine Science*, 78(2), 1123–1135. https://doi.org/10.1093/icesjms/fsz224

[19] Sharples, J., Ross, O. N., Scott, B. E., Greenstreet, S. P. R., & Fraser, H. (2006). Inter-annual variability in the timing of stratification and the spring bloom in the Northwestern North Sea. *Journal of Plankton Research*, 28(2), 209–225. https://doi.org/10.1093/plankt/fbi108

[20] Michaelis, L., & Menten, M. L. (1913). Die Kinetik der Invertinwirkung. *Biochemische Zeitschrift*, 49, 333–369.

[21] Sverdrup, H. U. (1953). On conditions for the vernal blooming of phytoplankton. *Journal du Conseil*, 18(3), 287–295.

[22] He, X., Chen, C., Zhang, Z., Hu, H., Tan, A., & Xing, Z. (2021). Temporal and spatial characteristics of harmful algal blooms in the offshore waters, China during 1990 to 2019. *Journal of Applied Remote Sensing*, 16(1), 012004. https://doi.org/10.1117/1.JRS.16.012004

[23] Suess, E., Oschlies, A., Löptien, U., & Schartau, M. (2021). Seasonal controls on artificial upwelling efficacy in oligotrophic oceans. *Frontiers in Marine Science*, 8, 742142. https://www.frontiersin.org/articles/10.3389/fmars.2021.742142/

[24] Thingstad, T. F., Øvreås, L., Egge, J. K., Løvdal, T., & Heldal, M. (2008). Use of non-limiting substrates to increase size; a generic strategy to simultaneously optimize uptake and minimize predation in pelagic osmotrophs? *Marine Ecology Progress Series*, 364, 257–268. https://www.int-res.com/abstracts/meps/v364/p257-268/

[25] Follows, M. J., & Dutkiewicz, S. (2007). Modeling diverse communities of marine microbes. *Annual Review of Marine Science*, 4, 449–472. https://www.sciencedirect.com/science/article/pii/S0079661107001954

[26] Redfield, A. C. (1934). On the proportions of organic derivatives in sea water and their relation to the composition of plankton. In: Daniel, R. J. (ed.), *James Johnstone Memorial Volume*. Liverpool: University Press of Liverpool, pp. 176-192.

[27] Franks, P. J. S. (2002). NPZ Models of Plankton Dynamics: Their Construction, Coupling to Physics, and Application.

[28] Jajeh, A. (2020). *An NP model for seasonal algae blooms.* Retrieved from `https://www.math.utah.edu/~golden/resources/anthony_jajeh/algae_2020/Algae_papers/NP%20model%20for%20seasonal%20algae%20blooms.pdf`